Proc. Natl. Acad. Sci. USA
Vol. 92, pp. 796–800, January 1995
Medical Sciences

In situ detection, by spin trapping, of hydroxyl radical markers produced from ionizing radiation in the tumor of a living mouse

HOWARD J. HALPERN*†, CHENG YU*‡, EUGENE BARTH*, MIROSLAV PERIC*§, AND GERALD M. ROSEN¶‖

*Department of Radiation and Cellular Oncology, University of Chicago, Chicago, IL 60637; ¶Department of Pharmaceutical Sciences, Program in Pharmacology and Toxicology, University of Maryland School of Pharmacy, Baltimore, MD 21201; and ‖Research Service, Veterans Affairs Medical Center, Baltimore, MD 21201

Communicated by U. Fano, The James Franck Institute, The University of Chicago, Chicago, IL, October 3, 1994 (received for review June 17, 1994)

ABSTRACT **Hydroxyl radicals are thought to be responsible for the toxicity associated with ionizing radiation in tissues. Measurements of hydroxyl radicals generated by ionizing radiation in cellular systems have failed thus far to elucidate higher-level homeostatic responses to this and other reactive oxygen species. Careful assessment of prior indirect hydroxyl radical assays in living tissues indicates that they are prone to a variety of artifacts, making all but the most qualitative relationships difficult to establish. This paper describes the detection of hydroxyl radicals produced during radiation in the leg tumor of a living mouse, where the free radicals evolve; detection uses low-frequency electron paramagnetic resonance in combination with *in vivo* spin trapping. To our knowledge, this is the first report of such a direct measurement of free radical production in the tissues of a living animal.**

Ionizing radiation generates hydroxyl radicals from water through a process involving at least two steps. The highest-yield products are commonly characterized as follows (1)

$$H_2O + h\nu \rightarrow H_2O^{\ddagger} + e^- (\rightarrow e^-_{aq})$$

$$H_2O^{\ddagger} + H_2O \rightarrow HO\cdot + H_3O^+$$

Although similar events are believed to occur in living tissues exposed to ionizing radiation, biochemical homeostatic mechanisms affect the neutralization of free radicals before they can exert their effects (2, 3). Elucidation of supracellular aspects of these pathways requires direct quantitation of hydroxyl radical and other free radicals in living tissues. For example, does radiation-induced hyperemia lead to an increase or decrease in the production of hydroxyl radicals in a subsequent radiation dose? Tissue measurements of these effects are necessary to bridge the gap between cellular and animal models in assessing the biological effects of ionizing radiation and the physiologic responses to this oxidant stress.

The substantial technical difficulties involved have previously prevented direct measurements of hydroxyl radicals in living tissue. The problem, simply stated, lies in detecting, in a living system, a free radical that reacts with everything it comes in contact with at near diffusion-controlled rates. Biochemical assays—including ethylene generation by hydroxyl radical with methional (4), methane formation from reaction with dimethyl sulfoxide (5), or the production of carbon dioxide from hydroxyl reaction with benzoate (6)—are impossible in living tissue and problematic *in vitro*. The production of 8-hydroxyguanine in tissue extracts or its monitoring in the urine of living animals is a nonspecific marker of oxidative stress since the presence of other mutagens not directly associated with hydroxyl radical production (7–9) may give the same result. The same holds for thiobarbituric acid-reacting substances (10). For the better part of a decade, we have refined techniques to allow the detection of free radicals in living animals (11–13), and now we report our initial *in vivo in situ* experiments detecting free radicals we believe are derived from hydroxyl radicals produced in an irradiated tumor of a living mouse.

Among the available methods for identifying free radicals, spin trapping and detection with EPR spectroscopy has received considerable attention (14–17). An EPR-silent nitrone or nitroso compound reacting with an initial unstable free radical forms a relatively long-lived nitroxide free radical adduct—thus trapping the electron's unpaired moment—which can be directly observed in turbid solutions with EPR spectroscopy at ambient temperature (18–23). Spin trapping offers the opportunity to measure and distinguish simultaneously among a variety of important biologically generated free radicals. However, conventional X-band EPR spectroscopy is sensitive to free radicals only to within the first millimeter of the surface of living tissue (24). Techniques to overcome this limitation—rapid freezing (25), sample grinding (26, 27), chemical extraction of spin-trapped adducts (28), or measurements in bile (29, 30) or blood (31) obtained from living animals—are subject to artifacts that may mask the underlying physiology. The key to detecting free radicals directly in living tissue is based on developing an EPR spectroscopy capable of identifying these species deep in either human or animal tissues (12).

Detection of free radicals deep in human tissues and tumors requires resorting to much lower frequencies than are available with the conventional 10-GHz X-band spectrometer, namely, in the range of 100 to 300 MHz (32–34). To achieve tissue penetration and free radical detection in human organs we chose to develop *ab initio* a low-frequency EPR spectrometer (12). The frequency used, 250 MHz, permits measuring free radicals at a depth of 7 cm in tissue (12, 32–34), thereby allowing detection of radicals in the tissue where they evolve. This approach minimizes artifacts affecting techniques with conventional X-band EPR spectrometers. Recently we reported the use of spin trapping to image and identify hydroxyl radicals produced by ionizing radiation in 10-ml volumes of buffered solutions (35). These solutions mimic the difficult spectroscopic penetrability of living tissue. The same low-frequency—250-MHz—spectrometer described here and 5,5-

The publication costs of this article were defrayed in part by page charge payment. This article must therefore be hereby marked "*advertisement*" in accordance with 18 U.S.C. §1734 solely to indicate this fact.

Abbreviations: DMPO, 5,5-dimethyl-1-pyrroline 1-oxide; 4-POBN, α-(4-pyridyl 1-oxide)-*N*-*tert*-butylnitrone; 4-POBN-CH(OH)CH_3, α-hydroxyethyl-(4-pyridyl 1-oxide)methyl-*N*-*tert*-butyl nitroxide; DTPA, diethylenetriaminepentaacetic acid.

†To whom reprint requests should be addressed.
‡Present address: Norris Cancer Research Institute, Department of Radiation Oncology, 1441 East Lake Avenue, Los Angeles, CA 90033.
§Present address: Department of Physics and Astronomy, California State University at Northridge, 18111 Nordhoff Street, Northridge, CA 91330.

diperdeuteromethyl-(2,3,3,4,4-$^2H_5$)-1-pyrroline 1-oxide (DMPO-d_{11}) and 5,5-dimethyl-(2,3,3-$^2H_3$)-1-pyrroline 1-oxide (DMPO-d_3) spin traps were used. Deuteration simplified the spectral signature (DMPO-d_3), and full deuteration (DMPO-d_{11}) increased the signal intensity. This allowed the definition of the Breit–Rabi spectroscopic shifts in the spectra of spin-trap adducts and their detection with as little as 15 Gy of radiation. These studies established the possibility of *in vivo* spin trapping (35).

Spin trapping *in vivo* is restricted by the modest signal from low-frequency EPR and by the low concentration of free radicals whose biologic half-life is limited (35). Deuteration of the spin trap enhances the sensitivity toward superoxide and hydroxyl radicals, but the stability of the spin-trap adducts seems insufficient to allow their identification in the reductive environment of living tissues (35, 36). However, recent reports (37, 38) suggested that nitroxides, derived from the spin trapping of alkyl free radicals by α-phenyl-*N*-*tert*-butylnitrone (PBN), might be stable *in vivo*, thereby increasing the cumulative nitroxide concentration. We determined that addition of excess ethanol to an hydroxyl radical-generating system produces α-hydroxyethyl radicals (39). In the presence of α-(4-pyridyl 1-oxide)-*N*-*tert*-butylnitrone (4-POBN), we observed an EPR spectrum characteristic of α-hydroxyethyl-(4-pyridyl 1-oxide)methyl-*N*-*tert*-butyl nitroxide [4-POBN-CH(OH)-CH_3] (40, 41). This reaction appears specific for the hydroxyl radical. The second-order rate constant for the reaction of α-hydroxyethyl with 4-POBN was calculated to be 3.1×10^7 $M^{-1}\cdot s^{-1}$ (41). In addition, 4-POBN-CH(OH)CH_3 displayed remarkable stability, appearing to be relatively unaffected by the presence of high fluxes of superoxide and of other potential redox-active agents (40). Finally, the 4-POBN/EtOH spin-trapping system proves to be 10 times more sensitive to hydroxyl radical formation than is DMPO/EtOH (41), thus serving as an excellent spin-trapping system to detect hydroxyl radical which might evolve from the radiation of a murine tumor in a living mouse. We chose an extremity tumor system for these initial experiments to deliver high, toxic doses of radiation to a substantial bulk of tissue with minimal effect on the physiology of the rest of the animal.

MATERIALS AND METHODS

Materials. Diethylenetriaminepentaacetic acid (DTPA) was purchased from Sigma. Monobasic and dibasic sodium phosphate were purchased from J. T. Baker. Buffers were passed through a column loaded with Chelex 100 from Bio-Rad. They were titrated to a pH of 7.8 and adjusted to a concentration of 50 mM. Reagent grade ethyl alcohol (200 proof) was purchased from Midwest Grain Products (Pekin, IL); (1-^{13}C)ethyl alcohol ($CH_3{}^{13}CH_3OH$) was purchased from Cambridge Isotope Laboratories (Cambridge, MA); and 4-POBN was purchased from Aldrich and used without further purification. 3-Trimethylaminomethyl-2,2,5,5-tetramethyl-1-pyrrolidinyloxyl iodide was synthesized according to the methods of S. Pou, P. L. Davis, G. L. Wolf, and G.M.R. (unpublished results). Use of the chelator DTPA and eliminating metal ions from buffers with Chelex 100 ensured the stability of our spin-trapping solutions before their use.

Instrumental Conditions. A low-frequency EPR spectrometer previously described (22) was operated at 260 MHz (g = 2 field of 93 G). At this frequency, the skin depth (37% sensitivity) is approximately 7 cm of tissue. The spectrometer consists of a lumped-circuit parallel inductance and capacitance resonator, with a single-turn inductance provided by the sample holder. The balanced capacitive coupling, adjustable electronically, allows correcting for animal motion and microphonic-induced variations in the coupling over frequency ranges of several hundred Hz. The resonator for these experiments was fabricated from ABS plastic resin GPX 3700 (General Electric) electroplated with copper and gold (General Superplating, East Syracuse, NY). Its sensitive volume consists of a cylinder 1.5 cm thick and 1.6 cm in diameter. This volume is just sufficient to accommodate the mouse leg and its tumor. The resonator characteristics provide, for the mouse leg and tumor, a radiofrequency magnetic field (B_1) of 0.27 G, with a power of 15 mW, at a loaded Q (quality factor) of approximately 180. The modulation frequency was 5.12 kHz, with a field amplitude of 1.2 G. Data acquisition was accomplished under the control of a microcomputer. Spectra were obtained with 246 points per scan, 2 scans per spectrum. The time constant and point acquisition time were 0.1 s, yielding a spectral acquisition time of approximately 1 min.

Model Sample Preparation. To a 0.75-ml sample of 50 mM sodium phosphate buffer 4-POBN (250 mM), ethyl alcohol (0.85 M), and DTPA (1 mM) were added and subjected to 3000 Gy of radiation from a Gammacell 220 ^{60}Co small volume radiator (AECL, Ville de Lavalle, PQ, Canada) at a dose rate of 2.1 Gy/s. The sample was exposed in a polyethylene vial and transferred to a second vial that partially (approximately 25% by volume) filled the resonator installed in the low-frequency EPR spectrometer. A second sample was prepared as above but substituting (1-^{13}C)ethyl alcohol for natural-abundance ethyl alcohol.

Mouse Tumor Radiation Conditions. The tumor model in these experiments was the NFSa fibrosarcoma (42), whose initial cells were kindly provided by Catherine Mason and Luka Milas of the M. D. Anderson Hospital, Houston. Cells ($0.5–1.0 \times 10^6$) were implanted subcutaneously in the legs of C3H mice and grown to a diameter of 12 mm. For all experiments, the tumor-bearing C3H/sed mouse was anesthetized with diazepam (20 mg/kg) and ketamine (45 mg/kg) for irradiation and spectral acquisition. Several experiments were performed with 3-trimethylaminomethyl-2,2,5,5-tetramethyl-1-pyrrolidinyloxyl iodide to monitor the efflux from the tumor of a stable nitroxide compound with a pharmacologic compartmental distribution similar to that of 4-POBN-CH(OH)CH_3. On the basis of octanol partition coefficients (see below) both this nitroxide and the spin-trap adduct appear to be quite hydrophillic. A volume of 0.2 ml of 30 mM solution of this nitroxide was injected directly into the tumor and spectra were obtained. The spin-trapping solution consisted of 50 mM sodium phosphate buffer with 500 mM 4-POBN, 1.7 M ethyl alcohol, and 1 mM DTPA. A volume of 0.23 ml of the spin-trapping solution was injected intratumorally in 30 s with very modest loss, less than 0.04 ml. For one group of experiments monitoring the nitroxide efflux from a tumor after intratumoral injections and for experiments with the spin-trapping solution, a tourniquet of 0-silk suture was applied to the leg proximal to the tumor and pulled tight 50 s after the start of the intratumoral injection. The mouse was placed in a Gammacell 220 ^{60}Co radiator producing a dose of 2.1 ± 0.2 Gy/s at the tumor. A cylinder of lead and Cerrobend (lead/tin/bismuth alloy) shielded the mouse, reducing the dose to its body by a factor of 40 (5.3 half-value layers). End caps on the shield were split and a half circle was hollowed from each side, allowing passage of the mouse thigh. The exposed tumor was wrapped in 0.5 cm of tissue-equivalent material (Superflab; Alimed, Dedham, MA) to allow dose build up. Air was circulated in the radiator during irradiation. The mouse did not lie directly on metal surfaces. Prior measurements under similar conditions indicate the mouse core temperature to have remained above 32°C. Radiation began 5 min after the injection began. The exposure lasted 23 min and 48 s, producing a dose of 3000 ± 300 Gy.

Tumor Spectral Acquisition Conditions. For tumor radiation measurements, the spectrometer was roughly tuned with the anesthetized mouse in place and its tumor was centered in the resonator prior to spin-trap injection and tumor radiation. Thus, the spectral sensitivity is localized to the heavily irradi-

ated tumor and the leg in the immediate vicinity. The mouse was gently restrained in a special acrylic immobilization jig designed to mechanically decouple the living animal sample from the resonator. The elastoplast limb restraints also wrapped about pegs that fit tightly into holes in the jig, allowing a reproducible setup. After radiation, the mouse was transported from the radiator and its tumor was installed in the EPR resonator. Spectral acquisition began 8.5 min after the end of radiation. The mouse leg and tumor temperature was maintained at 37.0 ± 0.5°C by radiant heating from two opposed heat lamps.

Spectral Simulation. The EPR spectrum obtained from the radiated sample, including 4-POBN and the natural-abundance carbon ethyl alcohol in buffer, was simulated with a spectral model consisting of six lines each (a nitrogen triplet and β-hydrogen doublet), as the spectrum expected from 4-POBN-CH(OH)CH_3. Each line consisted of a weighted sum of Lorentzian and Gaussian lines (90% Lorentzian, 10% Gaussian) with 1-G peak-to-peak linewidths. As detailed elsewhere (35), low-frequency spectra display large Breit–Rabi shifts in the individual spectral line positions relative to spectra obtained at high frequency. These shifts were evaluated by using the full Breit–Rabi hyperfine matrix. Because the cumbersome Breit–Rabi matrix solutions made iterative fitting difficult for the actual splittings with given hyperfine constants, the goodness-of-fit of the simulation was judged by eye. A 12-line spectrum describes the 4-POBN-^{13}CH(OH)-CH_3 [α-hydroxy-(α-^{13}C)ethyl-(4-pyridyl 1-oxide)methyl-*N*-*tert*-butyl nitroxide] spectrum with the additional α-^{13}C splitting. A 25% Gaussian component for each 1-G linewidth gave an optimal fit.

Octanol Partition Coefficient Measurement. HPLC-grade water (J. T. Baker) was mixed with EtOH (5% and 10%, vol/vol) and 4-POBN (250 and 500 mM, respectively) and the two solutions were irradiated to 3000 Gy. The resulting solutions were separated into two samples each. Spectra from one of each subsamples were obtained from a standard X-band spectrometer (JEOL JESME-1X) operated at 1-mW power, 0.5-G modulation field, 100-kHz modulation frequency, and a time constant of 1 s, requiring 4 min for a 50-G field sweep. The second subsample was mixed 50% vol/vol with octanol and manually shaken in a beaker for 30 min. An identical volume of the water layer that formed in the beaker after shaking was used for EPR spectra. The heights of the spectra were measured. The octanol partition coefficient was the difference of the spectral heights divided by the height of the initial water sample. The octanol partition coefficient of the quaternary ammonium nitroxide was obtained similarly.

RESULTS AND DISCUSSION

The spectrum obtained from 4-POBN plus EtOH irradiated with 3000 Gy in buffer is shown in Fig. 1*A* above a simulation of the spectrum based on the hyperfine splitting constants A_N = 15.8 ± 0.1 G and A_H = 2.5 ± 0.1 G, which is consistent with those obtained at conventional frequencies (X-band) for 4-POBN-CH(OH)CH_3 (A_N = 15.75 G and A_H = 2.4 G) (41). Substituting $CH_3{}^{13}CH_2OH$ for EtOH in the above reaction produced the spectrum of Fig. 1*B*, which is shown above a spectral simulation based on splitting constants A_N = 15.8 ± 0.1 G, A_H = 2.5 ± 0.1 G, and A_{13C} = 4.0 ± 0.2 G. Again, these are consistent with X-band measurements (A_N = 15.75 G, A_H = 2.4 G, and A_{13C} = 3.75 G) of a 4-POBN/$CH_3{}^{13}CH_2OH$ sample subjected to hydroxyl radicals produced in an entirely different fashion (41). This substitution verifies that the spectrum from the irradiated solution obtained from EtOH/4-POBN arises from (*i*) the reaction of hydroxyl with EtOH to give α-hydroxyethyl radical and (*ii*) the spin trapping of α-hydroxyethyl radical by 4-POBN. In buffer, the half-life of 4-POBN-CH(OH)CH_3 signal was found to be 9 days. We

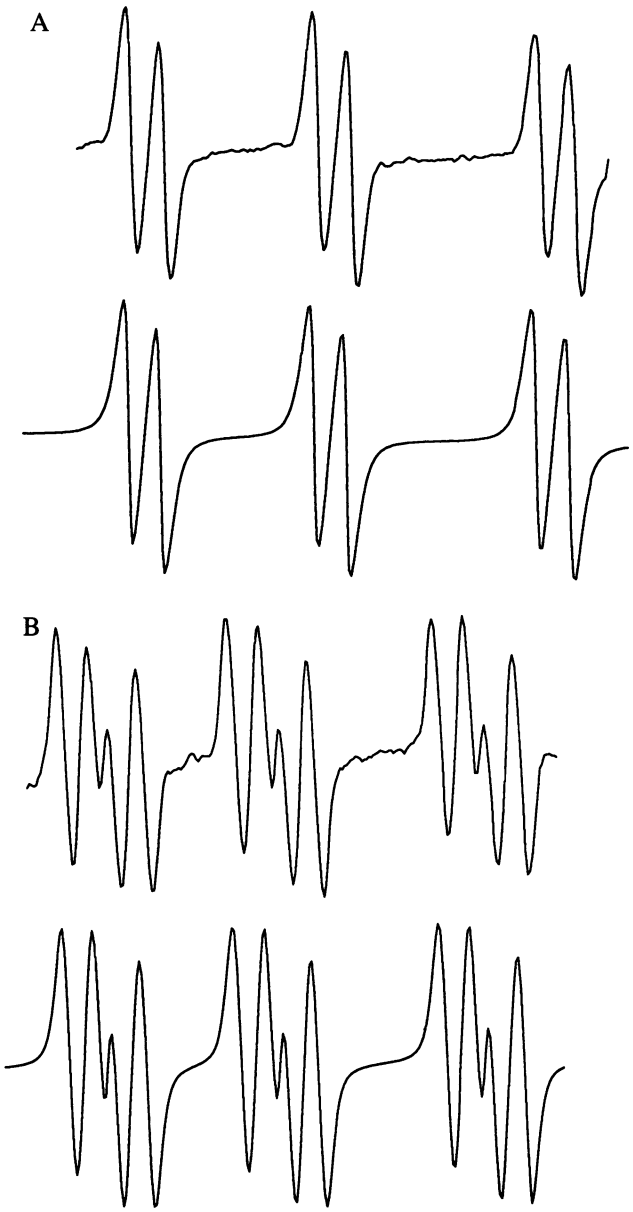

FIG. 1. (*A*) Low-frequency EPR spectrum from 4-POBN/5% EtOH/1 mM DTPA in sodium phosphate buffer subjected to 3000 Gy of γ radiation. Simulation of the data with literature hyperfine splitting constants (30) is shown under the spectral data. The best splitting constants were A_N = 15.8 ± 0.1 G and A_H = 2.5 ± 0.1 G, consistent with published values for the splittings for 4-POBN-CH(OH)CH_3: A_N = 15.75 G, A_H = 2.4 G (41). (*B*) Low-frequency EPR spectrum from a 1-ml sample prepared as described for *A* except that $CH_3{}^{13}CH_2OH$ was substituted for EtOH. Spectral acquisition was also under identical conditions. The simulation of the spectrum is shown below the spectral data. The splitting constants were A_N = 15.8 ± 0.1 G, A_H = 2.5 ± 0.1 G, and A_{13C} = 4.0 ± 0.3 G, again consistent with those previously published values at X-band: A_N = 15.75 G, A_H = 2.4 G, and A_{13C} = 3.75 G (41).

measured the octanol partition coefficient of 4-POBN-CH(OH)CH_3 to be 0.22 ± 0.01. That of the quaternary ammonium nitroxide was <0.02. Both are therefore hydrophilic.

In a series of preliminary experiments (data not shown) where the tumor was radiated with 3000 Gy, requiring approximately 25 min, no EPR signal was detected. We conjectured that once we injected 4-POBN into the tumor, rapid distribution from the site of injection made it difficult to detect

4-POBN-CH(OH)CH_3 in the tumor 25 min later. In other studies we were able to change the half-life of certain nitroxides in tissue perfusate by stopping perfusate flow (11). To determine whether a similar approach could help maintain the EPR signal in tissue for our *in vivo* studies, we injected a charged nitroxide (0.2 ml of 30 mM 3-trimethylaminomethyl-2,2,5,5-tetramethyl-1-pyrrolidinyloxyl iodide), whose octanol partition coefficient mimics that of 4-POBN-CH(OH)CH_3, into a 12-mm NFSa fibrosarcoma implanted in the leg of a C3H mouse. The signal half-life was found to be 8 min. However, a tourniquet, consisting of heavy surgical suture (0-silk) placed proximal to the tumor, increased the half-life to 35 min.

With the mouse anesthetized, a 12-mm tumor in the leg was injected directly with a solution (0.2 ml) of 4-POBN/EtOH (500 mM 4-POBN in 50 mM sodium phosphate buffer containing 1 mM DTPA and 1.7 M EtOH). The tourniquet was immediately applied to the leg just proximal to the tumor. The mouse was then fitted into its radiation shield, exposing only the leg containing the tumor, and the tumor was treated with 3000 Gy of radiation. After treatment, the tumor-bearing portion of the mouse leg was fitted into a resonator in the low-frequency EPR spectrometer (Fig. 2) and EPR spectra were recorded. The spectrum is shown in Fig. 3 with a simulation as in Fig. 1*A*. We continued to record spectra for another 20 min, until noise completely overwhelmed the characteristic signal of 4-POBN-CH(OH)CH_3. Radiation of the tumor in the absence of the 4-POBN/EtOH mixture failed to produce an EPR spectrum.

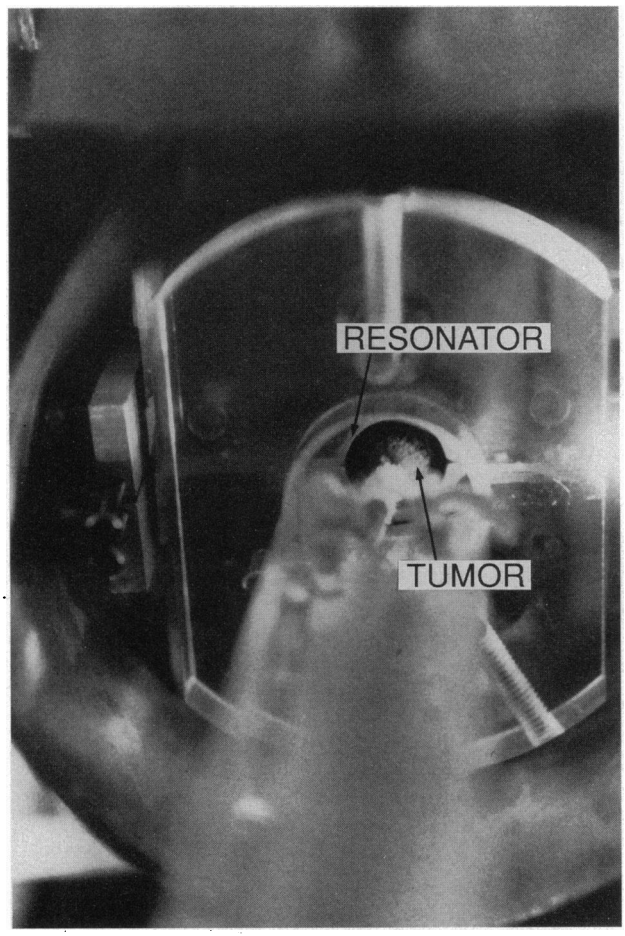

FIG. 2. Mouse leg tumor situated in the low-frequency EPR spectrometer resonator. With current immobilization the tumor could be reproducibly placed in the resonator, and spectral acquisition was begun 3 min after the animal was brought into the spectrometer room. An additional 2 min was necessary for animal transit.

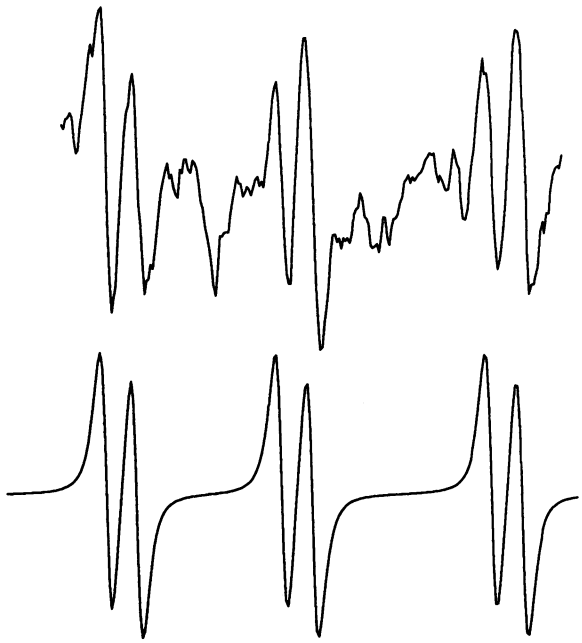

FIG. 3. Spectrum obtained from a 12-mm-diameter NFSa tumor in the leg of a mouse situated as shown in Fig. 2 in the resonator of the low-frequency EPR spectrometer. The tumor was injected with 0.2 ml of 4-POBN (500 mM)/EtOH (10%, vol/vol) in 50 mM sodium phosphate buffer, a tourniquet was applied proximal to the tumor, and the tumor was subjected to 3000 Gy of radiation over 24 min. The mouse was transported to the low-frequency EPR spectrometer and spectra were obtained under acquisition conditions described in the text. The lower trace is a simulation as described for Fig. 1*A*.

The acquisition of the spectral signal has involved administering extremely high doses of radiation—a total of 3000 Gy over 24 min. Using water G values for hydroxyl radical production, this dose corresponds the production of 36 μM hydroxyl radical per min, three orders of magnitude higher than the dose given in a single clinical fraction of radiation (43). Further work is necessary to optimize the trade-off between the increase in signal with increasing dose and the decay of the signal during the dose delivery time. Deuterated spin traps with increased signal per spin-trap adduct molecule should yield additional sensitivity. Most importantly, the current spectrometer operates at a frequency allowing detection of free radicals in tissues much larger than a 12-mm mouse leg tumor. At least two and possibly three orders of magnitude in sensitivity should be regained by operating with a correspondingly larger tumor sample.

Previous investigations, in which spin traps were injected into animals and isolated preparations from these animals were placed into conventional EPR spectrometers, set the stage for the studies reported in this communication. To our knowledge, this is the first time free radicals have been spin trapped *in vivo* and recorded *in situ* in a living animal. We recognize that the doses of radiation required to detect hydroxyl radicals in this mouse model were well above the therapeutic range used to kill tumors. Nevertheless, we view this work as a first step to the understanding of the important role free radicals play in many physiologic processes.

X-rays were discovered 99 years ago (44). Within a year they were applied to human breast cancer as a local toxin (45). They were soon found to be mutagens (46). Despite nearly a century of x-ray use as an antineoplastic agent and 57 years of its known role as a mutagen, the mechanisms of x-ray damage *in vivo* are a matter of debate. Part of this problem lies in the difficulty in

measuring putative intermediate steps in the cascade from radiation exposure to biologic effect. Determining the mechanisms and significance of free radical events will clearly require us to identify and quantitate these reactive species if, when, and where they evolve *in vivo.* Although much work remains to be done before specific free radicals are identified as the result of some physiologic or pathologic process, the spin-trapping/low-frequency EPR method presented here promises to become a powerful tool for the delineation of free radical mechanisms in biology.

We thank Dr. Ralph R. Weichselbaum for his support and enthusiasm and Dr. Michael K. Bowman for useful discussions. Janet Riley provided skill, effort, and patience in the preparation of the manuscript. This research was supported in part from National Institutes of Health Grants CA-50679 and HL-33550, The Balaban Foundation, the Veterans Affairs Research Service, and the Council for Tobacco Research–USA.

1. von Sonntag, C. (1987) *The Chemical Basis of Radiation Biology* (Taylor & Francis, London), pp. 31–34.
2. Howard-Flanders, P. (1970) *Adv. Biol. Med. Phys.* **13,** 553–603.
3. Alper, T. (1979) *Cellular Radiobiology* (Cambridge Univ. Press, Cambridge, U.K.).
4. Klebanoff, S. J. & Rosen, H. (1978) *J. Exp. Med.* **148,** 490–506.
5. Repine, J. E., Eaton, J. W., Anders, M. W., Hoidal, J. R. & Fox, R. B. (1979) *J. Clin. Invest.* **64,** 1642–1651.
6. Segone, A. L., Decker, M. A., Wells, R. M. & Democko, C. (1980) *Biochim. Biophys. Acta* **628,** 90–97.
7. Floyd, R. A. (1990) *Carcinogenesis* **11,** 1447–1450.
8. Kasai, H., Chung, M. H., Jones, D. S., Inoue, H., Ishikawa, H., Kamiya, H., Ohtuka, E. & Nishimura, S. (1991) *J. Toxicol. Sci.* **16,** Suppl., 95–105.
9. Ames, B. (1991) *Jpn. J. Cancer Res.* **82,** 1460–1461.
10. Mizumoto, Y., Nakae, D., Yoshiji, H., Andoh, N., Horiguchi, K., *et al.* (1994) *Carcinogenesis* **15,** 241–246.
11. Rosen, G. M., Halpern, H. J., Brunsting, L. A., Spencer, D. P., Strauss, K. E., Bowman, M. K. & Wechsler, A. S. (1988) *Proc. Natl. Acad. Sci. USA* **85,** 7772–7776.
12. Halpern, H. J., Bowman, M. K., Spencer, D. P., Van Polen, J., Dowey, E. M., Massoth, R. J., Nelson, A. C. & Teicher, B. A. (1989) *Rev. Sci. Instrum.* **60,** 1040–1050.
13. Halpern, H. J., Peric, M., Nguyen, T. D., Bowman, M. K., Lin, Y. J. & Teicher, B. A. (1991) *Phys. Med.* **7,** 39–45.
14. Iwamura, M. & Inamoto, N. (1967) *Bull. Chem. Soc. Jpn.* **40,** 702–703.
15. Iwamura, M. & Inamoto, N. (1970) *Bull. Chem. Soc. Jpn.* **43,** 856–860.
16. Janzen, E. G. & Blackburn, B. J. (1968) *J. Am. Chem. Soc.* **90,** 5909–5910.
17. Janzen, E. G. & Blackburn, B. J. (1969) *J. Am. Chem. Soc.* **91,** 4481–4490.
18. Janzen, E. G. (1971) *Acc. Chem. Res.* **4,** 31–40.
19. Finkelstein, E., Rosen, G. M. & Rauckman, E. J. (1980) *Arch. Biochem. Biophys.* **200,** 1–16.
20. Janzen, E. G. (1980) in *Free Radicals in Biology*, ed. Pryor, W. A. (Academic, New York), Vol. 4, pp. 116–154.
21. Rosen, G. M. & Finkelstein, E. (1985) *Free Radical Biol. Med.* **1,** 345–375.
22. Pou, S. D., Hassett, D. J., Britigan, B. E., Cohen, M. S. & Rosen, G. M. (1989) *Anal. Biochem.* **177,** 1–6.
23. Pou, S. & Rosen, G. M. (1990) *Anal. Biochem.* **190,** 321–325.
24. Poole, C. P. (1983) *Electron Spin Resonance: A Comprehensive Treatise on Experimental Techniques* (Wiley, New York), 2nd Ed.
25. Zweier, J. L., Flaherty, J. T. & Weisfeldt, M. L. (1987) *Proc. Natl. Acad. Sci. USA* **84,** 1404–1407.
26. Baker, J. E., Felix, C. C., Olinger, G. N. & Kalyanaraman, B. (1988) *Proc. Natl. Acad. Sci. USA* **85,** 2786–2789.
27. Nakazawa, H., Ichimori, K., Shinozaki, Y., Okino, H. & Hori, S. (1988) *Am. J. Physiol.* **255,** H213–H215.
28. Lai, E. K., Crossley, C., Rajagopalan, S., Missra, H. P., Janzen, E. G. & McKay, P. B. (1986) *Arch. Biochem. Biophys.* **244,** 156–160.
29. Burkitt, M. J. & Mason, R. P. (1991) *Proc. Natl. Acad. Sci. USA* **88,** 8440–8444.
30. Knecht, K. T. & Mason, R. P. (1993) *Arch. Biochem. Biophys.* **303,** 185–194.
31. Blasig, I. E., Ebert, B. & Love, H. (1986) *Stud. Biophys.* **116,** 35–42.
32. Bottomley, P. A. & Andrew, E. R. (1978) *Phys. Med. Biol.* **23,** 630–643.
33. Roschmann, P. (1987) *Med. Phys.* **14,** 922–931.
34. Hoult, D. I., Chen, C. N. & Sank, V. J. (1986) *Magn. Reson. Med.* **3,** 730–746.
35. Halpern, H. J., Pou, S., Peric, M., Yu, C., Barth, E. & Rosen, G. M. (1993) *J. Am. Chem. Soc.* **115,** 218–223.
36. Pou, S., Rosen, G. M., Wu, Y. & Keana, J. F. W. (1990) *J. Org. Chem.* **55,** 4438–4443.
37. Keana, J. F. W., Pou, S. & Rosen, G. M. (1989) *J. Org. Chem.* **54,** 2417–2420.
38. Samuni, A., Krishna, C. M., Reisz, P., Finkelstein, E. & Russo, A. (1989) *Free Radical Biol. Med.* **6,** 141–148.
39. Finkelstein, E., Rosen, G. M. & Rauckman, E. J. (1982) *Mol. Pharmacol.* **21,** 262–265.
40. Ramos, C. L., Pou, S., Britigan, B. E., Cohen, M. S. & Rosen, G. M. (1992) *J. Biol. Chem.* **267,** 8307–8312.
41. Pou, S., Ramos, C. L., Gladwell, T., Renks, E., Centra, M., Young, D., Cohen, M. S. & Rosen, G. M. (1994) *Anal. Biochem.* **217,** 76–83.
42. Milas, L., Wike, J., Hunter, N., Volpe, J. & Basic, I. (1987) *Cancer Res.* **47,** 1069–1075.
43. Hall, E. J. (1988) *Radiobiology for the Radiologist* (Lippincott, Philadelphia), 3rd Ed.
44. Röntgen, W. C. (1895) *Sitzungsber. Phys.-Med. Ges.* **9,** 132–141.
45. Grubbé, E. H. (1933) *Radiology* **21,** 156–162.
46. Muller, H. J. (1927) *Science* **66,** 84–87.